Evidence of spatial periodic firing in the subiculum of mice

P. Abad-Perez[1, 2], Scott R [3]. V. Borrell[2] , L. Martínez-Otero[2] , J.R. Brotons-Mas[1,2*]

[1] Universidad Cardenal Herrera-CEU, CEU Universities, Spain

[2] Instituto de Neurociencias UMH-CSIC. Alicante

[3] *Universidad de Alicante, Alicante*

*Corresponding author: Jorge R Brotons-Mas

e-mail: jorge.brotonsmas@uchceu.es; jbrotons@umh.es

Address: Universidad CEU Cardenal Herrera; Plaza Reyes Católicos, 19. 03204 Elche Alicante, Spain

Instituto de Neurociencias UMH-CSIC; Avd Ramón y Cajal SN, Edificio Ramón y Cajal, 03550,San Juan de Alicante, Alicante, Spain.

Abstract

The subiculum (SUB) is a region located at the core of the hippocampal formation. The SUB receives input from grid cells located in the medial entorhinal cortex (MEC) and from place cells in the CA1 area. Moreover, this structure mediates the output from the hippocampus to cortical and sub-cortical areas involved in the processing of different types of information. Despite the potential relevance of the SUB, its role in memory and spatial coding remains poorly studied. Previous work described a heterogeneous population of SUB spatial neurons, with evidence of its role in coding the geometry of the environment and spatial navigation in darkness. With the aim of further understanding the properties of spatial coding in the SUB, we implanted mice with microdrives carrying tetrodes to target CA1 and the SUB. Apart from the classical place cells described before, we discovered a fraction of SUB pyramidal neurons that generated spatial periodic firing. SUB spatial neurons presented lower spatial resolution and spatial stability than CA1 place cells. The role of spatial periodic neurons in the SUB might be relevant in several computations through the interaction of this region with CA1, the pre-parasubiculum and the MEC.

Keywords:

Spatial navigation, subiculum, place cells, grid cells, subiculum, hippocampus, periodic firing.

Significance Statement:

Spatial information coding and memory formation rely on a complex circuit involving the hippocampal formation and multiple types of spatially tuned neurons. For the first time, we found evidence of pyramidal neurons the SUB of mice exhibiting grid-like and periodic firing patterns. Our data support the idea that the SUB may play a role in complex spatial information processing, extending beyond the integration of CA1 unit inputs.

Introduction

Since the discovery of hippocampal place cells neurons that code for space by being active in specific locations of the environment (1) multiple efforts have aimed to understand the computational bases of spatial navigation. As a result, different types of spatially modulated neurons have been described across brain regions: head direction cells (HD); border and boundary vector cells (BVC), coding for the geometry of the environment in medial entorhinal cortex (MEC) and the SUB; and grid cells (GC) in the medial entorhinal cortex (MEC) (2–8). These neurons are either strongly involved in the codification of external information, such as BVC coding for geometry, or in egocentric related information. This is the case for grid cells (GC), where tessellating regular firing is associated with the representation of spatial metrics and is therefore essential for path integration—the ability to navigate in the absence of external cues (9). The integration of both allocentric and egocentric streams of information is instrumental in generating an efficient spatial representation.

Multiple computational models have sought to uncover the mechanisms underlying the integration of different types of spatial signals. The BVC model suggested that place cells require the existence of BVC neurons coding for the geometry of the environment (10). Other models suggested that place cells require GC activity (2,11). However, single unit recordings during neurodevelopment have demonstrated that HD, place cells and boundary neurons appear before GC during neurodevelopment (12,13). Thus, the dependence of place cells activity on grid cell firing seems to be unclear (14) .

Further research has considered the heterogeneity among different spatial cell types and their distributed anatomical localizations. In this context, the SUB may serve as a critical anatomical hub for spatial navigation (15,16). Strategically located between the EC and CA1, the SUB supports spatial information processing in a complex and heterogeneous manner. While spatial neurons in CA1 typically exhibit spatial reliability, the behavioral

correlates of SUB neuron activity include location, speed, direction, and the geometry of the spatial context, while also providing a reliable representation of space across light-dark transitions (17–20). Interestingly, the SUB is among the first areas affected in Alzheimer's diseases, it propagates epileptogenic activity in temporal lobe epilepsy (TLE) and is involved in schizophrenia (7,21–24). The SUB contains neurons with a diverse electrophysiological characteristic that might have different roles in memory process (25,26).

Previous work in rats indicated the existence of grid-like, spatially tuned activity in the SUB, attributed to axonal inputs from the MEC (8). This raised the possibility that SUB pyramidal neurons could integrate periodic signals from the EC and aperiodic signals from CA1. However, whether such grid-like activity originates from local SUB pyramidal neurons has not been extensively investigated until now. Here, we sought to test the presence of periodic firing in individual SUB cells of mice using large open-field arenas. We found evidence of grid-like and other forms of spatially periodic firing (i.e., band-like,(27)) in SUB neurons whose electrophysiological characteristics are compatible with pyramidal neurons**.** To the best of our knowledge, this is the first evidence of spatially periodic neurons in the rodent SUB, highlighting the unique role of this structure in shaping the spatial cognitive map.

Methods

Subjects

Male wild-type C57 mice, N=9, age p60 to p90 supplied by the UMH “Servicio de Experimentación Animal (SEA)" were used. Mice were maintained on a 12 h light/dark cycle with food and water available *ad libitum* and were individually housed after electrode implantation. All procedures were approved by the UMH-CSIC ethics committee, and the regional government, and they complied with local and European guidelines for animal experimentation (86/609/EEC).

In vivo recordings on freely moving mice.

Micro-drives (Axona Ltd.) equipped with four independent screws were loaded with tetrodes (12 mm tungsten wire, California Fine Wire Company, Grover Beach, CA, USA). Electrodes were implanted using isoflurane anesthesia and buprenorphine for analgesia, via a craniotomy performed above the hippocampus. Animals with misplaced electrodes or evidence of lesions were excluded from the analysis**.** Mice were recorded in standard arenas (50 x 50 cm) and larger open-field arenas (70 x 70 cm).

Data acquisition.

As in a previous studies (28) electrophysiological recordings were obtained using 16-channel headstage (gain x1), with an infrared light-emitting diode (LED) to track mouse position (Axona Ltd, UK). Signals were amplified (400 to 1000x), band pass filtered 0.3 Hz to 24 KHz, (Dacq system, Axona, UK) and recorded at 48 KHz/24 bit precision. These recordings were initially used to determine electrode location before the implementation of the recording protocols. For single unit recordings, the signal was band-pass filtered between 380 Hz and 6 KHz. Spikes were recorded whenever the signal was 3-4 times above background noise, typically 20-30 μV and stored in windows of 1 ms duration (200 ms before threshold and 800 ms after threshold detection). Spike waveforms were

sampled at 48 KHz while the same channels were also recorded in continuous mode at 4.8 KHz and band-pass filtered between 0-3-2.4 KHz.

Local field potential recordings.

During recording sessions, animals were examined for their basal activity while they were in their home cages. Ripple power, unit activity and theta power were used as electrophysiological landmarks to determine electrode location.

Place cells recordings.

Animals were recorded using the pellet chasing task. Small pellets of food were thrown in every 20 s to random locations within the open field, keeping the animal in continuous locomotion, thereby allowing a complete sampling of the environment.

Data Analysis.

Local field potential data was analyzed using custom-written MatLab codes (Mathworks, Natick, MA, USA). Raw recordings were FIR filtered (<1.2 KHz) and down sample to 2.4 KHz. Similar to previous studies (28,29) data obtained from open-field recordings was used to characterize the LFP. Running speed was computed based on the coordinates of the animal's position. To visualize the power spectrum in relationship to the speed of movement the spectral power (in decibels, 10log10) and spectrogram was built using the Thomson multi-taper method. A sliding window with 50% overlap, yielding a frequency resolution of 1 Hz was used.

Unit isolation and spike train analysis.

Single-unit activity was isolated using cluster-cutting techniques developed for data acquired with tetrodes, TINT (Axona, St. Albans, UK). Principal components, peak-to-trough distance, voltage at time t, peak height, trough, time of peak and time of trough in each electrode were used for unit isolation. Klustakwik was employed for initial cluster discrimination, followed by manual refinement based on principal components, spike

132 amplitude, and other parameters. To verify cluster quality isolation the probability of
133 cluster overlapping was calculated as described before (28,30). Spike trains were
134 analyzed by generating interval time histograms and temporal auto-correlogram. Only
135 units with no spikes in the refractory period of the inter-spike time histogram (1-2 ms),
136 and with spike amplitudes 3-4 times above background noise, typically 20-30 mV, were
137 included. Putative pyramidal cells and interneurons were distinguished based on
138 established criteria (8). Further spike train analysis was performed to determine the
139 bursting properties of the recorded neurons using the burst index (BI) proposed by Royer
140 and the propensity to burst (PrtB) proposed by Staff (31,32).

141 Firing rate maps.

142 Firing-rate maps were assembled as described previously. Pixel maps were converted
143 to a bin matrix with a bin size of 2.5 cm x 2.5 cm. Firing rate in each bin was determined
144 by a smoothing process using overlapping squares of 7.5 cm x 7.5 cm as described
145 before. Firing fields were plotted as a contour map reflecting the frequency of firing;
146 colors were interpolated from the top firing bins down to the lowest firing area by scaling
147 them in decreasing intervals of the peak firing and giving them a color scale: red highest
148 frequency, dark blue, lowest frequency. The spatial information content was quantified
149 using the Skaggs information indexes for the smoothed map (33) .

150 Spatial coherence, a spatial autocorrelation measurement**,** was calculated as the
151 correlation coefficient between the firing rate of each bin and the average rate of its eight
152 surrounding bins (34). Firing fields were defined as a group of 6 contiguous bins, where
153 the firing frequency was above the mean firing frequency plus the standard error of the
154 firing matrix. The maximal firing frequency of this group of bins had to be above 1 Hz.
155 For those units displaying more than one firing field, firing field size was computed as
156 the sum of the existing firing fields and expressed as the percentage of the arena size
157 occupied by the firing field calculated using the smoothed firing matrix. In-field maximum
158 frequency was computed as the maximum firing field frequency of the smoothed firing

map. Mean frequency was computed as the total number of spikes divided by the total recording time to provide the average session firing rate expressed in Hz.

To classify units as having spatially related activity, a randomized distribution was calculated by circular shifting the spikes times vs the position. This strategy allowed us to generate a random distribution without affecting the temporal firing structure of neurons (13). The values obtained in the original unsmoothed firing map and respecting the position matrix (n=1000). For a unit to be regarded as being spatially modulated, it had to display a spatial coherence above 99% of the randomized distribution. This same random distribution was used to obtain stability index between the original and a random distribution. Thus, for units to be regarded as stable they had to be above the 99% of cross-correlation between the original and the randomized distribution.

Grid analyses and periodic firing analysis.

Grid analyses were implemented following similar criteria to previous studies (2). Spatial autocorrelograms were calculated for each firing map.

$$r(\tau_x,\tau_y)=\frac{n\sum\lambda(x,y)\lambda(x-\tau_x,y-\tau_y)-\sum\lambda(x,y)\sum\lambda(x,y)\sum\lambda(x-\tau_x,y-\tau_y)}{\sqrt{n\sum\lambda(x,y)^2-(\sum\lambda(x,y))^2}\sqrt{n\sum\lambda(x-\tau_x,y-\tau_y)^2-(\sum\lambda(x-\tau_x,y-\tau_y))^2}}$$

where r is the autocorrelation between the original firing rate map and its spatially shifted copy. The lag τ is normally 1-dimensional for signal analysis. Because of the 2-dimensional nature of the firing rate map, the autocorrelation has lags in the x- and y-directions: τx and τy. n is equal to the number of pixels. To determine the existence of a hexagonal grid firing structure, grid index, size and orientation were calculated as described previously.

To obtain the “gridness index” we obtained a circular portion of the spatial autocorrelogram generated from the spatial firing matrix. This circle was centered on the central peak which was eliminated from the matrix. Then we correlated the rotated versions, in steps of 6º , of this matrix with the original spatial autocorrelogram. The

184 degree of spatial periodicity (‘gridness’ or ‘grid scores’) was determined for each
185 recorded cell and the grid index calculated as previously described (35).

186 Periodic Firing

187 Then we obtain the sum of values of the 2D resulting map in all its orientation and we
188 displayed the preferred orientation of these neurons in space as a polar plot (27). These
189 values were plotted against the polar plot of the shuffled original firing map, n=1000. Only
190 neurons that showed higher values than this confidence interval were considered as
191 periodic neurons.

192 Histological Analysis

193 After completing experiments, animals were sacrificed using sodium pentobarbital (180
194 mg/kg at a concentration of 100 mg/ml) and transcardially perfused with saline and 4%
195 paraformaldehyde. This procedure was authorized by the ethical commission according
196 to the current normative and following veterinary recommendations. The brains were
197 removed, sliced in 40 µm sections, and prepared for Immunohistochemistry against
198 DAPI, NeuN (Merck,ltd) and GFAP (Adigene technologies) for electrode localization.

199 Statistical analysis

200 Distribution of dependent variables was tested for normality and for equal variance.
201 Parametric statistical tests were used for normally distributed variables and non-
202 parametric tests were used for variables that did not show normal distribution. All
203 descriptive values are expressed as mean ± the standard error (S.E.). Statistical
204 significance was set at $p < 0.05$. All statistical analysis was performed using SPSS (IBM,
205 V27) software package.

206 # Results

207 To test for the presence of spatially periodic SUB cells, we performed recordings in
208 standard (50 x 50 cm) and large open fields (70x70cm), relative to the mouse body size
209 (6-8 cm). Postmortem analysis confirmed the placement of three tetrodes in the SUB
210 region, (see Fig 1A). A total of 147 CA1 and 65 subicular neurons were recorded in eight
211 mice (five implanted in the CA1 area, one in the subiculum and two in both regions).
212 Units were classified based on their spike duration, waveform shape and firing frequency
213 (Fig 1B), as previously reported (7). We isolated 74 CA1 and 28 SUB cells that meet
214 pyramidal and spatially modulation criteria (see methods) and were further analyzed.

215 First, we verified that there was no difference in the sorting quality across isolated units
216 in both regions (CA1 vs SUB: Overlapping probability 0.06±0.01 vs 0.10±0.02;
217 U=4290.0, p=0.236, Mann-Whitney), (28,30). Then, we looked for differences in the
218 basic electrophysiological properties, including spike amplitude, duration, and firing rate.
219 Statistical analysis indicated similar spike amplitude and duration (Fig 1B). Neither there
220 were differences for spike amplitude nor the duration (CA1 vs SUB: spike duration
221 477.53±7.8 μs vs. 491.02±10.39 μs: U=862.0, p=0.192; spike amplitude 254.1±11.9 μv
222 vs 226.07±15.6 μv: U=943.0, p=0.48) (Fig.1C, D). Instead, we observed significant
223 higher firing rate for SUB neurons (mean firing frequency; 1.2±0.12 Hz vs. 1.8±0.2 Hz:
224 U=745.0, p=0.02, Mann-Whitney) (Fig.1E). These results were consistent with previous
225 descriptions in rats and in mice (7,18,36). Further, no difference was found for the spike
226 duration between SUB spatial and non-spatial neurons (p=0.108), indicating that these
227 units were not axons coming from the MEC.

228 The interaction between the CA1 and the SUB is critical for the organization of inputs
229 and outputs of the hippocampal formation. This dialog depends on the specific timing of
230 the activity of different populations of neurons in different theta cycle windows (37).
231 Therefore, examining the relationship between CA1 and SUB firing and local LFP is

232 fundamental to understanding the temporal dynamics of the hippocampal formation. We
233 investigated the relationship between the firing of CA1 and SUB neurons with the locally
234 recorded theta (4-12Hz). We found that CA1 neurons showed a bimodal distribution
235 accumulating neurons in the ascending and descending phases of the local theta
236 oscillations (Fig.1F). In contrast, SUB neurons showed a higher concentration around
237 the peak of the locally recorded theta (Fig.1G).

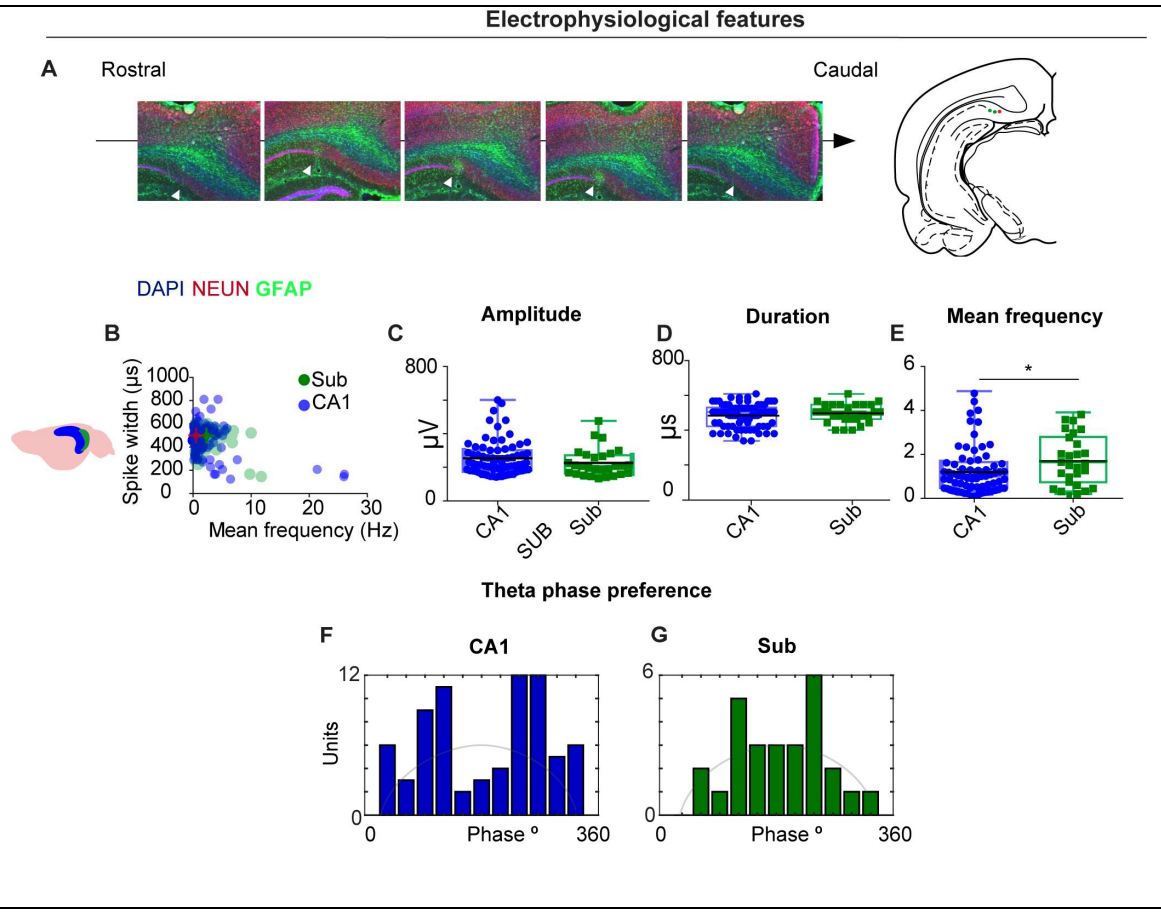

Figure 1. Electrophysiological properties of CA1 and SUB recorded units. **A.** Electrode location indicated by GFAP signal in the proximal SUB. Slices ordered from rostral to caudal. **B** Red dots indicate electrode locations. **B.** Scatter plot of spike width and firing rate for CA1 and SUB. Most units presented pyramidal-like properties. Red and green crosses represent the electrophysiological properties of units in figure 2. **C** and **D**. No significant differences were found for spike amplitude and spike duration between both regions. **E.** Firing rate was significantly higher for SUB units. **F** and **G**. Phase firing preference of theta in CA1 and SUB. Values indicate a bimodal distribution in CA1 and a more concentrate firing of SUB neurons around the peak of theta

238

239 A group of subicular neurons showed grid and spatially periodic firing

240 In rats, spatial representation in the SUB has typically been defined by a heterogeneous
241 population of place cells and boundary vector cells (BVC) (5,8). Given the larger size of
242 rats compared to the typically used arenas, detecting spatially periodic cells was likely
243 challenging. In contrast, using 50 x 50 cm arenas for mice, we observed that many SUB
244 neurons displayed significant recurrent firing at specific spatial orientations. Remarkably,
245 and in contrast to previous reports (8) , these units presented clear electrophysiological
246 characteristics of pyramidal neurons (Fig 2A,B), fired consistently along the entire
247 session (Fig.2C), and could not be confounded with another overlapping cell (Fig.2D).
248 To quantify periodicity, we performed a 2D Fourier transform of the unsmoothed firing
249 fields and calculated the orientation and number of modules (27). We found that about
250 14% of SUB spatial (four units) units met grid index criteria (Fig.2C-E). CA1 pyramidal
251 units recorded in the very same arenas did not exhibit these trends (Fig.2A' to F').

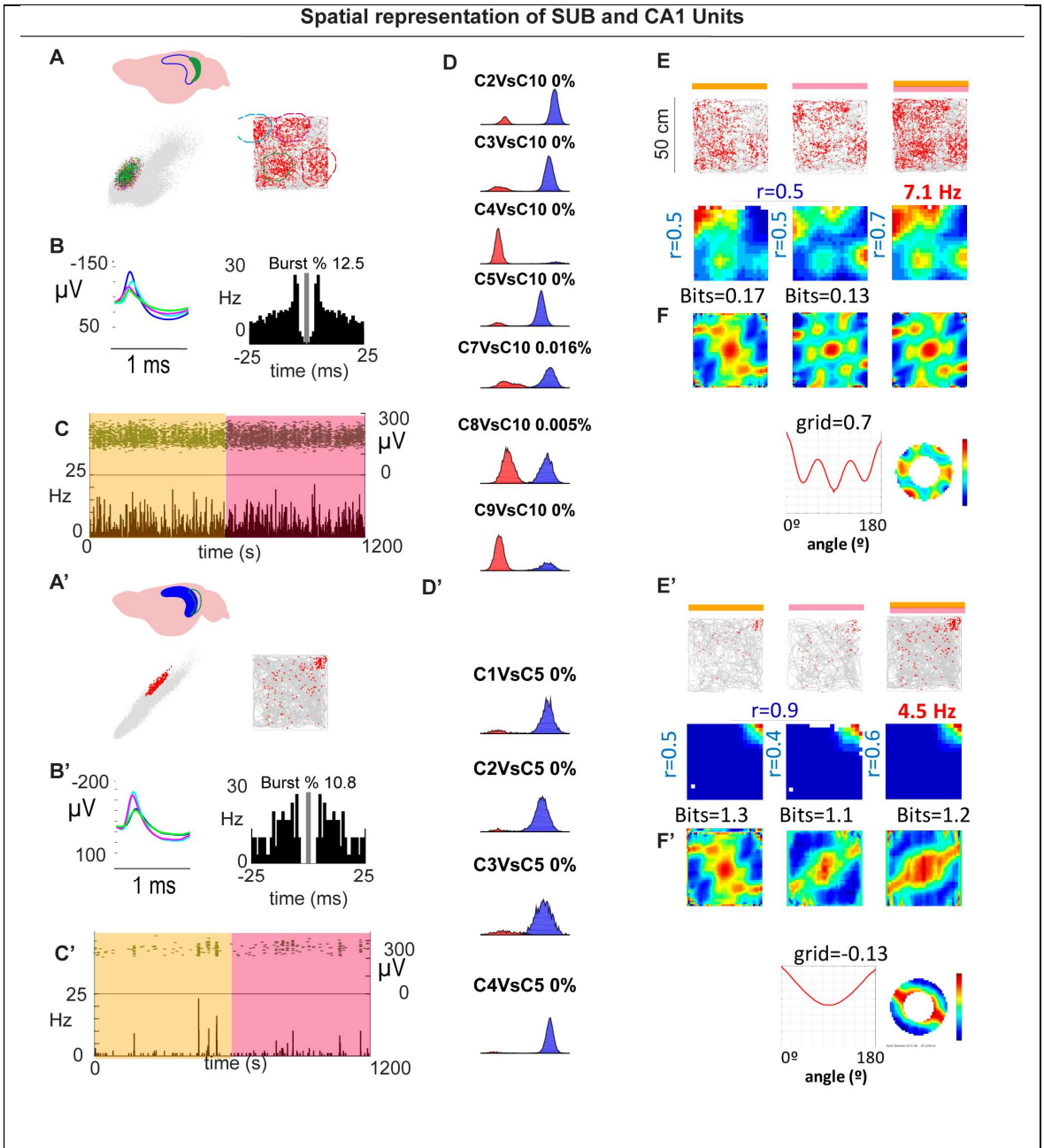

Figure 2. Spatial firing of SUB and CA1 units. **A** and **B.** An isolated units recorded in the SUB region of a mouse exploring a 50 x 50 cm arena. Multiple peaks in the firing field were contained in the same cluster. Notice different colors in the cluster and in the spike position figure. Waveform of the isolated unit and spike autocorrelogram indicated that this unit was consistent with a pyramidal cell with tendency to fire in burst and with a clean refractory period. **C**. Spike amplitude during the 20 min recording session in the open field 50x50 cm. It can be noticed how the spike properties were stable during the recording. Bottom panel in C indicates the instant firing rate during exploration. The two different colored shadows indicate the two halves represented later in E. **D**. Probability of overlapping unit in A, unit C10 vs other simultaneously recorded units. **E.**

Top panel shows the tracking of the mice, gray lines. Red dots represent the position of the mouse when the unit was active. Data was segmented in the two halves, orange, and pink shadows as in C. The full recording is showed at most right panel. Bottom panel represents the firing frequency matrix. Stability for the two halves was calculated, (r=0.5). Spatial coherence, light blue text color, and maximal firing rate, red text color. **F.** Spatial autocorrelograms helped to reveal the spatial regularity of some units. Bottom panel shows grid index calculation, met by this unit. **A'** to **F'** represent the same information for a unit recorded in the CA1 region. **A'** and **B'**: Note that while the CA1 unit firing frequency was lower than that of the SUB unit shown above, their electrophysiological properties were similar: wide spikes, clean autocorrelograms and propensity to burst.

253 We examined the identification of spatially periodic SUB cells by testing their responses
254 in arenas of different dimensions. To do this, we longitudinally tracked a subset of
255 individual SUB cells across 50x50 cm and 70x70 cm square boxes, and found consistent
256 grid-like responses (Fig.3A,B versus A',B'). Additionally, several SUB neurons that
257 showed discrete place fields in the 50 x 50 cm arena changed their firing generating
258 periodic firing in the large arena (Fig.3C,D versus C',D').

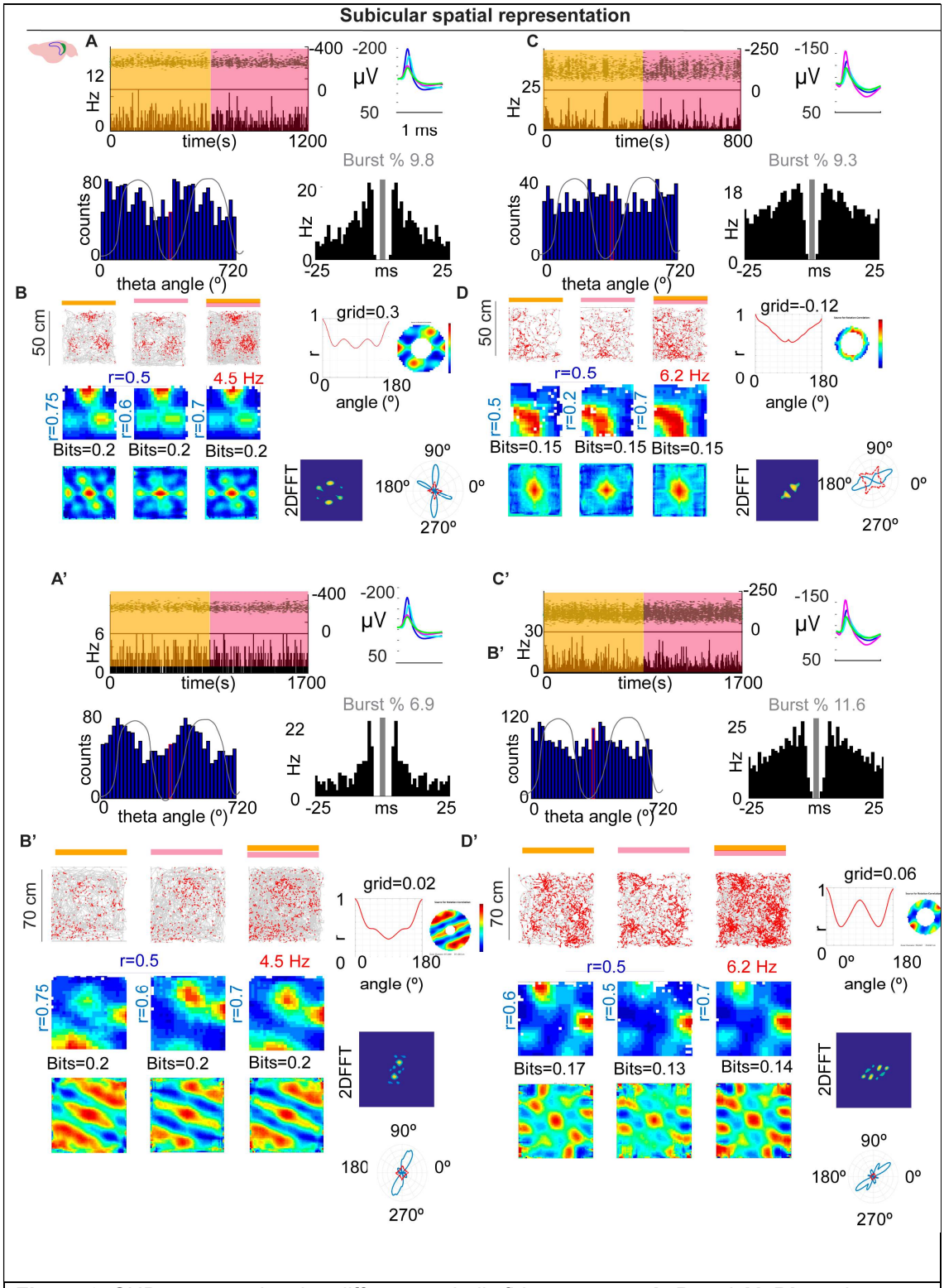

Figure 3. SUB neurons showing different periodic firing patterns. **A, B** and **A', B'** are the same recorded unit in a 50x50 cm arena and then in a 70x70cm arena. This unit showed stable characteristics in both conditions, see spike amplitude in first panel in **A** and **A'**. See, waveform similarity in both recordings, top right panel in A and A'. This neuron tended to fire in the ascending phase of theta and presented a clear bursting activity, see bottom panels in A and

A'. **B.** Neuron in this panel displayed a clear grid firing in the 50 x50 cm arena. However, this grid-firing pattern changed in the 70x70 cm arena. The autocorrelogram and the 2D FFT showed that this unit tended to fire in a periodic manner in space. See **B'** most left panels including the 2D FFT and the polar plot derived from this analysis. Blue represents the sum of values of the 2D FFT and the red line the same values for a randomized distribution, n=1000, of the original firing matrix. **C, D** and **C', D'** another SUB unit that did not showed grid firing in the 50x 50 cm arena. However, when the experiment was performed in the 70x70cm arena, a non-grid periodic firing emerged.

Spatial firing of SUB neurons showed lower spatial modulation than CA1

As previously mentioned, spatial coding in the hippocampal formation exhibits differential spatial characteristics across regions (19,38). To confirm functional specificity of SUB neurons, we next investigated their spatial characteristics as compared with those of CA1 units using standard parameters such as the spatial information per second and per spike, the spatial coherence, and the firing field size. We found significant differences between CA1 and SUB neurons for the spatial information per second, spatial information per spike, and for the spatial coherence (Fig.3A-C), consistent with previous reports. In contrast, no significant differences were observed for the firing field size (CA1 vs SUB : bits/s 0.39±0.01 vs. 0.322±0.06 μs,: U=738.0, p=0.025; bits/spike 0.43±0.04 vs. 0.32±0.06: U=611.0, p=0.001, Mann-Whitney; spatial coherence: (r), 0.61±0.01 vs. 0.54±0.02: $t_{(100)=}$2.442, p=0.016; firing field size (%), 29.02±0.7 vs. 30.0±1.14, $t_{(100)=}$2.442, p=0.016).

A critical element for the representation of space is the stability of the spatial code in the temporal domain. This ensures consistent spatial tuning during different exploratory episodes, while integrating information about the temporal aspects of experience. Importantly, temporal instability may be associated with different trends for rate remapping (39), potentially confounding the detection of spatially periodic signals. To

278 address this, we investigated the temporal consistency of the spatial code along the
279 CA1/SUB axis. We divided each recording session into two halves of 10 min and then
280 we calculated the bin-by-bin, spatial correlation (Fig 3E). We observed that place cells in
281 the CA1 region showed significantly higher spatial consistency (CA1 vs SUB: intra trial
282 stability coherence (r), 0.72±0.02 vs. 0.61±0.04: U=764.0, p=0.041, Mann-Whitney).
283 However, periodic neurons showed high stability within each trial, (See Fig 3), ruling out
284 remapping effects as a confounding factor in the identification of spatially-periodic firing.

285

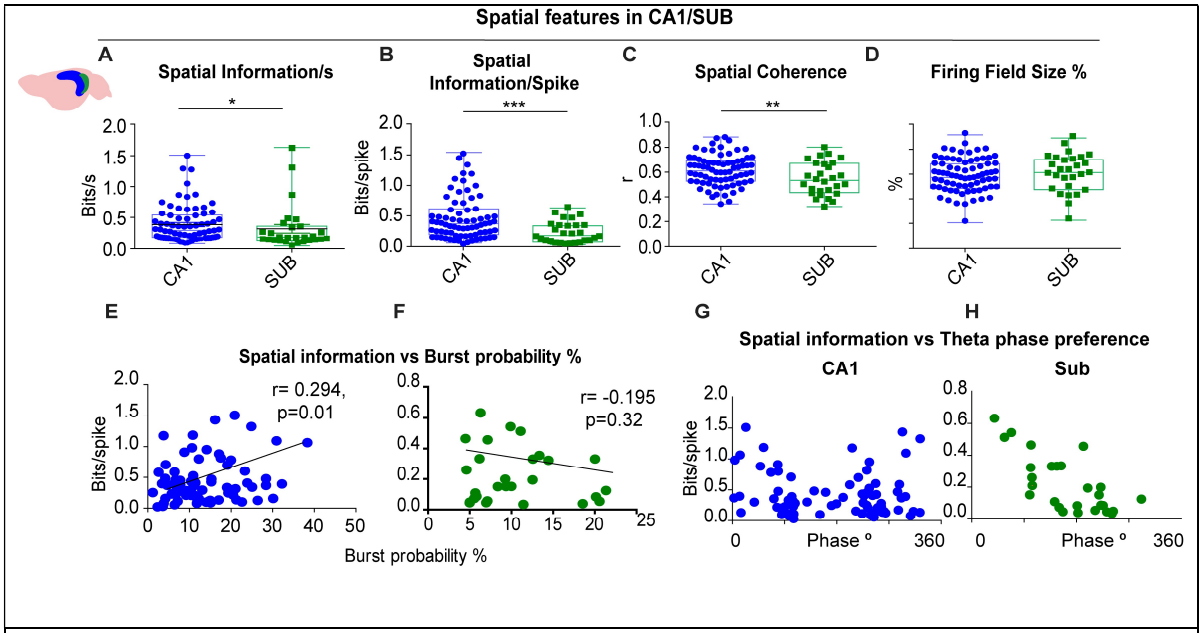

Figure 4. A to D. Different spatial parameters of SUB and CA1 units. **E** and **F** show the correlation between bursting activity and spatial information per spike. Results indicated a significant correlation for these variables only in the CA1 region. **G** and **H**. Spatial information of units in relationship to their preferred firing phase.

286

287 ## Spatial modulation of SUB units was not determined by bursting activity.

288 The spatial information code is related is closely related to the electrophysiological
289 characteristics of hippocampal pyramidal neurons. Specifically, place cells are known to
290 exhibit complex spikes, or bursting activity, which is characterized by the generation of
291 trains of action potentials within an envelope of 15-20 msec. This bursting pattern is

292 thought to increase enhance the fidelity of spatial information across different brain
293 regions (40). To investigate this, we sought to determine if there was a specific
294 relationship between bursting patterns and the spatial modulation in the CA1/SUB axis.

295 We observed that place cells in the CA1 region showed a significant correlation between
296 their bursting characteristics and the spatial modulation (Fig.4F,F'). Specifically, the
297 probability to burst was significantly correlated with the spatial information per second,
298 per spike and with the spatial coherence (PrtB vs bits per second, r= 0.485, p=0.0000;
299 PrtB vs bits per spike r= 0.294, p=0.01; PrtB vs spatial coherence, r= 0.35, p=0.002;
300 PrtB). Interestingly, the propensity to burst was also positively correlated with the mean
301 vector length, indicating that bursting propensity was associated with a stronger
302 relationship between units' activity and the ongoing locally recorded theta (PrtB vs mean
303 vector length, r= 0.35, p=0.002). A similar pattern emerged when we compared the
304 bursting index with the spatial modulation (BI vs bits per second, r= 0.26, p=0.026; BI vs
305 bits per spike r= 0.305, p=0.008; BI vs spatial coherence, r= 0.213, p=0.068; BI vs mean
306 vector length, r= 0.4, p=0.0005).

307 Remarkably, we observed no correlation between bursting properties and spatial
308 modulation in SUB-recorded units (PrtB vs bits per second, r= 0.274, p=0.158; PrtB vs
309 bits per spike r= -0.195, p=0.321; PrtB vs spatial coherence, r= -0.72, p=0.715; PrtB vs
310 mean vector length, r= 0.009, p=0.96). A similar pattern was observed when we
311 compared the bursting index with the spatial modulation (BI vs bits per second, -0.122,
312 p=0.573; BI vs bits per spike r= -0.210, p=0.283; BI vs spatial coherence, r= -0.257,
313 p=0.187; BI vs mean vector length, r= 0.009, p=0.96).

314 This indicates that CA1 neurons with a higher tendency to burst exhibited greater spatial
315 modulation, whereas in SUB-recorded neurons, bursting activity did not predict spatial
316 modulation, whether periodic or not.

Next, we investigated the specific phase of maximal information transfer. Remarkably, CA1 cells showed a non-linear relation between their preferred theta-firing phase and the spatial information (CA1 angular mean vs bits per second, r= -0.154, p=0.19; angular mean vs bits per spike r= -0.098, p=0.407; angular mean vs spatial coherence, r= -0.185, p=0.115), while SUB cells rather exhibited a negative linear correlation (Fig.4H,H'). This suggests that neurons with a preferred phase around the ascending phase of theta exhibited higher spatial information per spike (SUB angular mean vs bits per second, r= -0.429, p=0.023; angular mean vs bits per spike r= -0.581, p=0.001; angular mean vs spatial coherence, r= -0.519, p=0.005).

326 # Discussion

327 Here, we report for the first-time evidence of grid and spatially periodic firing of pyramidal
328 neurons in mice SUB. Recorded neurons fired at different phases of the ongoing theta
329 and their electrophysiological properties did not correlate with their spatiality. We verified
330 the quality of unit sorting by observing the significance of refractory period contamination
331 and calculating the overlapping probability of different clusters (30), finding no statistical
332 difference between isolated neurons in CA1 and SUB and meeting similar quality indices
333 as in relevant previous work (27,30,41). Moreover, spike waveforms clearly meet
334 pyramidal neuron characteristics and differ from potentially axonal recordings (42).

335 ## The role of periodic firing in the SUB in spatial cognition

336 Speed and direction of movement are critical for path integration, and both inputs have
337 been proposed as essential for grid cells. This could be provided by GC ensembles (43).
338 From a mechanistic perspective, the computation of speed may rely on theta oscillations,
339 which are strongly correlated with velocity, as well as on speed cells (44–48). Moreover,
340 the direction of movement is of great relevance (49). This directional input may be
341 provided by axis cells described in the SUB (50). Complementary to these inputs, the
342 speed and directional signals could also be shaped by periodic cells in the MEC, pre-
343 parasubiculum and SUB units reported here (50,51). The redundancy of different speeds
344 and direction inputs might provide a more robust spatial integration for the navigation
345 across different conditions, for example across light-dark transitions.

346 Our new evidence of spatially periodic cells suggests that the SUB may contribute to
347 generating spatial representations by supporting periodic cells and GC in the pre-
348 parasubiculum and MEC. This is supported by anatomical data that confirms the strong
349 afferences sent by the SUB to the pre- and parasubiculum and the deep layers of the
350 MEC (16,52). Additionally, the SUB might provide input from boundary vector cells (BVC)
351 and periodic neurons to hippocampal place cells through its back projection to the CA1

352 area (53). In this way, circuits involving SUB-MEC, SUB-CA1, might support the
353 transformation of the grid produced by alterations of the geometry of space (54). Finally,
354 SUB spatial representation appears to depend on thalamic inputs and might meditate
355 changes in GC due to thalamic lesions also known to be relevant for GC in MEC (55).

356 SUB spatial representation is different to CA1

357 We observed that place cells in the CA1 showed higher spatial resolution as compared
358 to SUB cells. This apparent lower spatial modulation of SUB neurons is related to their
359 higher firing rate. Such augmented activity seems to serve as a mechanism to improve
360 information routing from the hippocampal formation to other brain regions, a hypothesis
361 sustained by the anatomical location and connections of the SUB with other brain regions
362 (56). SUB neurons seem capable of maintaining active information during the inter-trial
363 in a working memory task (57). This same activity, or changes on this sustained activity,
364 might be relevant for the signaling of the temporal aspects of different episodes. The
365 integration of the what-when information by the same group of neurons would reflect
366 changes in their spatial activity across time. However, this hypothesis would need
367 specific experiments, to pinpoint the existence of the temporal coding by SUB neurons.

368 SUB neurons tended to fire across different phases of the LFP but clustered towards the
369 center of the theta cycle. This is at odds to previous reports that showed a higher
370 concentration towards the descending phase of theta and earlier than CA1 neurons (56).
371 This might be the result of different electrode location of the reference electrode at the
372 proximo-distal and deep-superficial layer. The fact that in this work we used tetrodes and
373 not multisite electrodes limits our capability to determine the deep-superficial location of
374 the recorded cells. Interestingly, neurons that fired in the earlier theta phases were more
375 strongly spatially modulated. As previously described, this is coherent with a specific
376 temporal organization for different types of information transfer across the theta cycle to
377 different brain structures (56).

Data limitation and context of the results

One of the caveats of our results is the low number of reported neurons and the existence of grid like firing in two of the mice. However, despite the low number of reported neurons, the recordings were consistent throughout the full experiment and met quality criteria for sorting methods. Moreover, in one implant, the recovery of the anatomy was not total, and the tip of the electrode was not clearly seen. However, electrode was estimated to have reached the subiculum by the presence of ripple activity. However, it might be possible that in this case the electrode drifted towards adjacent structures, such as the pre-subiculum etc. where ripples are also present (58). Thus, our results found consistency of a small number of neurons that showed periodic firing.

Conclusion

Here we present evidence of spatial periodic firing in the SUB. However, the properties, response to complex spatial manipulation or their relationship with BVC, GC and place need to be determined. The SUB is of great relevance for the integration of the spatial code, episodic memory and dimensions related to the ongoing tasks. Further work should aim to investigate the role of the SUB in memory consolidation and spatial coding and in other cognitive processes.

Author Contributions:

JRBM designed the experiments. JRBM and PA implemented the experiments, developed and implemented the analysis toolbox. VB and LM supported the project providing resources for its development and discussed the results. JBRM wrote the paper, and the manuscript was further reviewed, and data discussed by JBR, PA and RS.

Acknowledgments

We would like to thank Liset Menendez de la Prida and Professor Antonio Falcó for their comments on this manuscript and their unconditional support to our work.

Moreover, we want to thank Jim Donnett (Axona LTD) who was always available to help us with his technical support.

Funding: This project was supported by the Spanish State Research Agency, “Ministerio de Ciencia, Innovación y Universidades” (RTI2018-097474-A-100) obtained by JRBM, as well as by the UCHCEU (“Programa de Consolidación de Indicadores, AYUDAS PUENTE, Ayudas a grupos consolidados (GIR), GIR23/11.).

PA was funded by the UCHCEU-Banco de Santander fellowship.

VB was supported by grants from the European Research Council (309633) and the Spanish State Research Agency (PGC2018-102172-B-I00, as well as through the “Severo Ochoa" Programme for Centers of Excellence in R&D, ref. SEV-2017-0723).

The funders had no role in study design, data collection and analysis, decision to publish, or preparation of the manuscript.

416 ***References***

417 1. O'Keefe J, Dostrovsky J. The hippocampus as a spatial map. Preliminary evidence
418 from unit activity in the freely-moving rat. Brain Res [Internet]. 1971 Nov 12
419 [cited 2021 Dec 9];34(1):171–5.

420 2. Hafting T, Fyhn M, Molden S, Moser MB, Moser EI. Microstructure of a spatial
421 map in the entorhinal cortex. Nature. 2005 Aug 11;436(7052):801–6.

422 3. Fyhn M, Hafting T, Witter MP, Moser EI, Moser MB. Grid cells in mice.
423 Hippocampus. 2008 Dec;18(12):1230–8.

424 4. Taube JS, Muller RU, Ranck JB. Head-direction cells recorded from the
425 postsubiculum in freely moving rats. I. Description and quantitative analysis. J
426 Neurosci. 1990;10(2):420–35.

427 5. Lever C, Burton S, Jeewajee A, O'Keefe J, Burgess N. Boundary Vector Cells in the
428 Subiculum of the Hippocampal Formation. The Journal of Neuroscience. 2009
429 Aug 8;29(31):9771.

430 6. Solstad T, Boccara CN, Kropff E, Moser MB, Moser EI. Representation of
431 geometric borders in the entorhinal cortex. Science. 2008 Dec
432 19;322(5909):1865–8.

433 7. Sharp PE, Green C. Spatial correlates of firing patterns of single cells in the
434 subiculum of the freely moving rat. J Neurosci. 1994;14(4):2339–56.

435 8. Brotons-Mas JR, Schaffelhofer S, Guger C, O'Mara SM, Sanchez-Vives M V.
436 Heterogeneous spatial representation by different subpopulations of neurons in
437 the subiculum. Neuroscience. 2017 Feb 20;343:174–89.

438 9. McNaughton BL, Battaglia FP, Jensen O, Moser EI, Moser MB. Path integration
439 and the neural basis of the "cognitive map." Nat Rev Neurosci [Internet]. 2006
440 Aug [cited 2024 Nov 20];7(8):663–78.

441 10. Hartley T, Burgess N, Lever C, Cacucci F, O'keefe J. Modeling Place Fields in
442 Terms of the Cortical Inputs to the Hippocampus. 2000;

443 11. O'Keefe J, Burgess N. Dual phase and rate coding in hippocampal place cells:
444 Theoretical significance and relationship to entorhinal grid cells. Hippocampus.
445 2005;15(7):853–66.

446 12. Wills TJ, Cacucci F, Burgess N, O'Keefe J. Development of the hippocampal
447 cognitive map in preweanling rats. Science (1979). 2010 Jun 18;328(5985):1573–
448 6.

449 13. Langston RF, Ainge JA, Couey JJ, Canto CB, Bjerknes TL, Witter MP, et al.
450 Development of the spatial representation system in the rat. Science (1979).
451 2010 Jun 18;328(5985):1576–80.

452 14. Morris G, Derdikman D. The chicken and egg problem of grid cells and place
453 cells. Trends Cogn Sci [Internet]. 2023 Feb 1 [cited 2024 Jun 13];27(2):125–38.

454 15. Aggleton JP, Christiansen K. The subiculum: The heart of the extended
455 hippocampal system. Prog Brain Res. 2015;219:65–82.

456 16. O'Mara SM, Sanchez-Vives M V., Brotons-Mas JR, O'Hare E. Roles for the
457 subiculum in spatial information processing, memory, motivation and the
458 temporal control of behaviour. Prog Neuropsychopharmacol Biol Psychiatry.
459 2009 Aug 1;33(5):782–90.

460 17. Sharp PE. Subicular cells generate similar spatial firing patterns in two
461 geometrically and visually distinctive environments: Comparison with
462 hippocampal place cells. Behavioural Brain Research. 1997 Apr;85(1):71–92.

463 18. Brotons-Mas JR, Montejo N, O'Mara SM, Sanchez-Vives M V. Stability of
464 subicular place fields across multiple light and dark transitions. European Journal
465 of Neuroscience. 2010 Aug;32(4):648–58.

466 19. Barnes CA, McNaughton BL, Mizumori SJY, Leonard BW, Lin LH. Chapter 21
467 Chapter Comparison of spatial and temporal characteristics of neuronal activity
468 in sequential stages of hippocampal processing. Prog Brain Res. 1990 Jan
469 1;83(C):287–300.

470 20. Ledergerber D, Battistin C, Blackstad JS, Gardner RJ, Witter MP, Moser MB, et al.
471 Task-dependent mixed selectivity in the subiculum. Cell Rep. 2021 May 25;35(8).

472 21. Carlesimo GA, Piras F, Orfei MD, Iorio M, Caltagirone C, Spalletta G. Atrophy of
473 presubiculum and subiculum is the earliest hippocampal anatomical marker of
474 Alzheimer's disease. Alzheimer's & Dementia : Diagnosis, Assessment & Disease
475 Monitoring. 2015;1(1):24.

476 22. Godsil BP, Kiss JP, Spedding M, Jay TM. The hippocampal-prefrontal pathway:
477 The weak link in psychiatric disorders? Vol. 23, European
478 Neuropsychopharmacology. Elsevier; 2013. p. 1165–81.

479 23. Stafstrom CE. The role of the subiculum in epilepsy and epileptogenesis. Epilepsy
480 Curr. 2005 Jul;5(4):121–9.

481 24. Rosoklija G, Toomayan G, Ellis SP, Keilp J, Mann JJ, Latov N, et al. Structural
482 abnormalities of subicular dendrites in subjects with schizophrenia and mood
483 disorders: preliminary findings. Arch Gen Psychiatry. 2000;57(4):349–56.

484 25. Eller J, Zarnadze S, Bäuerle P, Dugladze T, Gloveli T. Cell Type-Specific Separation
485 of Subicular Principal Neurons during Network Activities. 2015;

486 26. Jarsky T, Mady R, Kennedy B, Spruston N. Distribution of Bursting Neurons in the
487 CA1 Region and the Subiculum of the Rat Hippocampus. J Comp Neurol.
488 2008;506:535–47.

27. Krupic J, Burgess N, O'Keefe J. Neural representations of location composed of spatially periodic bands. Science (1979) [Internet]. 2012 Aug 17 [cited 2021 May 31];337(6096):853–7.

28. Del Pino I, Brotons-Mas JR, Marques-Smith A, Marighetto A, Frick A, Marín O, et al. Abnormal wiring of CCK+ basket cells disrupts spatial information coding. Nat Neurosci. 2017 Jun 1;20(6):784–92.

29. Del Pino I, García-Frigola C, Dehorter N, Brotons-Mas JR, Alvarez-Salvado E, MartínezdeLagrán M, et al. Erbb4 Deletion from Fast-Spiking Interneurons Causes Schizophrenia-like Phenotypes. Neuron. 2013 Sep 18;79(6):1152–68.

30. Hill DN, Mehta SB, Kleinfeld D. Quality Metrics to Accompany Spike Sorting of Extracellular Signals. 2011;

31. Royer S, Sirota A, Patel J, Buzsáki G. Distinct representations and theta dynamics in dorsal and ventral hippocampus. Journal of Neuroscience. 2010 Feb 3;30(5):1777–87.

32. Staff NP, Jung HY, Thiagarajan T, Yao M, Spruston N. Resting and active properties of pyramidal neurons in subiculum and CA1 of rat hippocampus. J Neurophysiol [Internet]. 2000 [cited 2024 Apr 20];84(5):2398–408.

33. Markus EJ, Barnes CA, Bruce $, Mcnaughton L, Gladden VL, Skaggs WE. Spatial Information Content and Reliability of Hippocampal CA1 Neurons: Effects of Visual Input. HIPPOCAMPUS. 1994;4(4):410–21.

34. Muller RU, Kubie JL. The effects of changes in the environment on the spatial firing of hippocampal complex-spike cells. J Neurosci. 1987;7(7):1951–68.

35. Sargolini F, Fyhn M, Hafting T, McNaughton BL, Witter MP, Moser MB, et al. Conjunctive representation of position, direction, and velocity in entorhinal cortex. Science (1979) [Internet]. 2006 May 5 [cited 2024 Aug 19];312(5774):758–62. Available from:

36. Mizuseki K, Kitanishi T. Oscillation-coordinated, noise-resistant information distribution via the subiculum. Curr Opin Neurobiol. 2022 Aug 1;75:102556.

37. Valero M, de la Prida LM. The hippocampus in depth: a sublayer-specific perspective of entorhinal–hippocampal function. Vol. 52, Current Opinion in Neurobiology; 2018. p. 107–14.

38. Oliva A, Fernández-Ruiz A, Buzsáki G, Berényi A. Spatial coding and physiological properties of hippocampal neurons in the Cornu Ammonis subregions. Hippocampus. 2016 Dec 1;26(12):1593–607.

39. Leutgeb S, Leutgeb JK, Barnes CA, Moser EI, McNaughton BL, Moser MB. Neuroscience: Independent codes for spatial and episodic memory in

hippocampal neuronal ensembles. Science (1979). 2005 Jul 22;309(5734):619–23.

40. Simonnet J, Brecht M. Burst firing and spatial coding in subicular principal cells. Journal of Neuroscience. 2019 May 8;39(19):3651–62.

41. Navratilova Z, Godfrey KB, McNaughton BL. Grids from bands, or bands from grids? An examination of the effects of single unit contamination on grid cell firing fields. J Neurophysiol. 2016 Feb 19;115(2):992–1002.

42. Robbins AA, Fox SE, Holmes GL, Scott RC, Barry JM. Short duration waveforms recorded extracellularly from freely moving rats are representative of axonal activity. Front Neural Circuits

43. Zutshi I, Leutgeb JK, Leutgeb S. Theta sequences of grid cell populations can provide a movement-direction signal. Curr Opin Behav Sci. 2017 Oct 1;17:147–54.

44. Kramis R, Vanderwolf CH, Bland BH. Two types of hippocampal rhythmical slow activity in both the rabbit and the rat: Relations to behavior and effects of atropine, diethyl ether, urethane, and pentobarbital. Exp Neurol. 1975 Oct 1;49(1):58–85.

45. Chen Z, Resnik E, McFarland JM, Sakmann B, Mehta MR. Speed Controls the Amplitude and Timing of the Hippocampal Gamma Rhythm. PLoS One. 2011;6(6):e21408.

46. Long LL, Hinman JR, Chen CM, Escabi MA, Chrobak JJ. Theta dynamics in rat: Speed and acceleration across the septotemporal axis. PLoS One. 2014 May 19;9(5).

47. Kropff E, Carmichael JE, Moser EI, Moser MB. Frequency of theta rhythm is controlled by acceleration, but not speed, in running rats. Neuron. 2021 Mar 17;109(6):1029-1039.e8.

48. Abad-Perez P, Molina-Payá FJ, Martínez-Otero L, Borrell V, Redondo RL, Brotons-Mas JR. Theta/gamma Co-modulation Disruption After NMDAr Blockade by MK-801 Is Associated with Spatial Working Memory Deficits in Mice. Neuroscience. 2023 May 21;519:162–76.

49. Raudies F, Brandon MP, Chapman GW, Hasselmo ME. Head direction is coded more strongly than movement direction in a population of entorhinal neurons. Brain Res. 2015 Sep 24;1621:355–67.

50. Olson JM, Tongprasearth K, Nitz DA. Subiculum neurons map the current axis of travel. Nat Neurosci. 2017 Feb 1;20(2):170–2.

51. Jeewajee A, Barry C, O'Keefe J, Burgess N. Grid cells and theta as oscillatory interference: Electrophysiological data from freely moving rats. Hippocampus. 2008 Dec;18(12):1175–85.

52. O'Mara SM, Commins S, Anderson M, Gigg J. The subiculum: A review of form, physiology and function. Prog Neurobiol. 2001;64(2):129–55.

53. Xu X, Sun Y, Holmes TC, López AJ. Noncanonical connections between the subiculum and hippocampal CA1. J Comp Neurol. 2016 Dec 1;524(17):3666–73.

54. Krupic J, Bauza M, Burton S, Barry C, O'Keefe J. Grid cell symmetry is shaped by environmental geometry. Nature. 2015 Feb 12;518(7538):232–5.

55. Frost BE, Cafalchio M, Martin SK, Islam N, Aggleton JP, O'mara SM. Spatial Coding in the Subiculum Requires Anterior Thalamic Inputs. J Neurosci. 2021 Jul 28;41(30):6511-652

56. Kitanishi T, Umaba R, Mizuseki K. Robust information routing by dorsal subiculum neurons. Sci Adv. 2021 Mar 1;7(11).

57. Deadwyler SA, Hampson RE. Differential but complementary mnemonic functions of the hippocampus and subiculum. Neuron. 2004 May 13;42(3):465–76.

58. Chrobak JJ, Buzsáki G. High-Frequency Oscillations in the Output Networks of the Hippocampal–Entorhinal Axis of the Freely Behaving Rat. Journal of Neuroscience. 1996 May 1 [cited 2024 Sep 9];16(9):3056–66.